

# Photo-induced increase of the superconducting coherence lengths in oxygen-deficient $\text{YBa}_2\text{Cu}_3\text{O}_x$ thin films

C. Stockinger<sup>1</sup>, G. Heine<sup>1</sup>, W. Markowitsch<sup>1,a</sup>, W. Lang<sup>1</sup>, R. Adam<sup>2</sup>, R. Sobolewski<sup>2,b</sup>, R. Rössler<sup>3</sup>, J.D. Pedarnig<sup>3</sup>, and D. Bäuerle<sup>3</sup>

<sup>1</sup> Institut für Materialphysik der Universität Wien, Kopernikusgasse 15, 1060 Wien, Austria

<sup>2</sup> Department of Electrical and Computer Engineering and Laboratory for Laser Energetics, University of Rochester, Rochester, NY 14627-023, USA

<sup>3</sup> Angewandte Physik, Johannes-Kepler-Universität Linz, 4040 Linz, Austria

Received 15 December 1999 and Received in final form 24 May 2000

**Abstract.**  $\text{YBa}_2\text{Cu}_3\text{O}_x$  ( $x \approx 6.6$ ) thin films were photodoped with white light at various temperatures from 70 K to 290 K. Before and after the excitation, the magnetoconductivity was measured in a magnetic field  $B = 0.5$  T, and the experimental results were fitted to the Aslamazov-Larkin theory of superconducting order-parameter fluctuations to determine the superconducting coherence lengths,  $\xi_c(0)$  and  $\xi_{ab}(0)$ . We observed that the photodoping process enhanced  $\xi_c(0)$  and  $\xi_{ab}(0)$  and that the amount increased with the photodoping temperature increase. On the other hand, the superconducting anisotropy  $\xi_{ab}(0)/\xi_c(0)$  decreased with increasing temperature. The photodoping effect enhances superconducting properties of partially oxygen-deficient  $\text{YBa}_2\text{Cu}_3\text{O}_x$  samples and is considerably increased by high doping temperatures.

**PACS.** 73.50.Jt Galvanomagnetic and other magnetotransport effects (including thermomagnetic effects) – 73.50.Pz Photoconduction and photovoltaic effects – 74.40.+k Fluctuations (noise, chaos, nonequilibrium superconductivity, localization, etc.)

## 1 Introduction

It has been previously shown that prolonged illumination of oxygen depleted  $\text{YBa}_2\text{Cu}_3\text{O}_x$  ( $x < 7$ ) samples with visible and UV radiation (“photodoping”) induces an excited state that is persistent at low temperatures and has lifetimes of hours at room temperature. This excited state shows a modified normal-state transport [1–5], as well as changed structural [6,7], optical [8], and Raman [9] properties. In metallic samples, also the superconducting properties are affected by the photodoping process, as shown by the photo-induced enhancement of the superconducting transition temperature  $T_c$  [2,10–12] and the increase of the coherence lengths [13]. In addition, it has been recently demonstrated that photodoping changes as well the out-of-plane resistivity [14] and the electrical anisotropy of  $\text{YBa}_2\text{Cu}_3\text{O}_x$  [15].

We have observed that several of the above photo-induced effects, including the  $T_c$  enhancement, the Hall coefficient, and the normal-state electrical anisotropy depend on temperature  $T_{\text{dop}}$ , at which the photodoping is performed [5,12,14]. Apparently, photodoping at different  $T_{\text{dop}}$  leads to excited states with different physical prop-

erties. This finding is most likely related to the instability of the lattice structure of oxygen-deficient  $\text{YBa}_2\text{Cu}_3\text{O}_x$  near room temperature, which was also demonstrated by the observation of long-term relaxation processes in insulating  $\text{YBa}_2\text{Cu}_3\text{O}_x$  after abrupt temperature changes of only about 20 K [6]. Such effects are usually attributed to oxygen-ordering processes within the CuO chains of  $\text{YBa}_2\text{Cu}_3\text{O}_x$ . On the other hand, photodoping is known to have also an impact on the lattice structure [6,7], and, obviously, it makes a considerable difference whether the photodoping is carried out at low temperatures, where the lattice structure is stable, or at high temperatures where the diffusion of atoms becomes important.

In view of the above results it is of great interest to measure how the observed  $T_{\text{dop}}$  dependence of photodoping affects the superconducting state of  $\text{YBa}_2\text{Cu}_3\text{O}_x$ . The enhancement of  $T_c$  indicates such behavior, but, since  $T_c$  is closely related to the free-carrier concentration, its enhancement may simply reflect the observed increase of the (normal-state) Hall number. In [13], we have shown that the Ginzburg-Landau coherence lengths at  $T = 0$ ,  $\xi_c(0)$  and  $\xi_{ab}(0)$ , are both *increased* by photodoping at  $T_{\text{dop}} = 150$  K, whereas the superconducting anisotropy  $\xi_{ab}(0)/\xi_c(0)$  is reduced. The aim of this paper is to perform systematic investigations of the impact of photodoping on  $\xi_c(0)$  and  $\xi_{ab}(0)$  at different  $T_{\text{dop}}$ . We will show that

<sup>a</sup> e-mail: wilhelm.markowitsch@univie.ac.at

<sup>b</sup> Also at the Institute of Physics, Polish Academy of Sciences, 02904 Warszawa, Poland

the coherence lengths as well as  $\xi_{ab}(0)/\xi_c(0)$  are functions of  $T_{\text{dop}}$ . Compared with normal-state transport parameters, the coherence lengths are less influenced by extrinsic properties, *e.g.*, defect concentrations, thus, our results give strong evidence that the electronic properties of the photo-excited  $\text{YBa}_2\text{Cu}_3\text{O}_x$  state are substantially influenced by  $T_{\text{dop}}$ .

## 2 Sample preparation and measurement techniques

For the present studies we used three  $\text{YBa}_2\text{Cu}_3\text{O}_x$  thin films belonging to the “60-K plateau” ( $x = 6.5\text{--}6.6$ ) prepared at two different laboratories. Two of the films (labeled R1 and R2 throughout this paper) were prepared by rf sputtering on  $\text{LaAlO}_3$ . The initial  $T_{c0} \approx 90$  K was reduced to about 51 to 53 K by heating the samples at  $400^\circ$  for 2 h in 20 mTorr of oxygen. Test structures suitable for electrical measurements were patterned by a laser inhibition technique. For more details of the preparation techniques see [5,12,16,17]. The third sample (Y10) was grown by pulsed-laser deposition on a “wedged” (off-axis)  $\text{SrTiO}_3$  substrate with a tilt angle of  $10^\circ$  [18–20]. During the deposition, the substrate was kept at  $760^\circ$  in an oxygen atmosphere of 0.2 mbar. After deposition, the film was annealed *in situ* for 100 min without changing the temperature and oxygen pressure.  $T_c$  of Y10 was 57 K. A cross-shaped test structure was fabricated by means of photo-lithography and wet chemical etching. Similar samples were previously used to measure the anisotropic properties of  $\text{YBa}_2\text{Cu}_3\text{O}_x$ , *e.g.*, the Seebeck coefficient [18] and the electrical conductivity [14]. The present work, however, deals only with the in-plane conductivity of the sample Y10.

The studied samples were photodoped for 25 hours at several temperatures from 70 K to 290 K using a 100-W quartz-tungsten halogen lamp as the light source. During the illumination, the samples were mounted in a temperature-controlled closed-cycle refrigerator on a cold finger, placed within an electromagnet. Excessive sample heating was prevented by a water-filter in the optical path. Before and after the photo-excitation, the  $\rho_{ab}$  vs.  $T$  characteristics were measured, using a standard 4-point method with a highly stable ac-current source and lock-in technique. The samples were slowly cooled down from the photodoping temperature to 40 K and, subsequently, warmed up to room temperature. During the temperature sweeps, a transverse magnetic field of  $B = 0.5$  T was periodically applied, and, at each temperature, the longitudinal and transverse (Hall) resistivities were measured in both polarities of the magnetic field as well as at  $B = 0$ . After each temperature sweep, the sample was kept at room temperature for 24 hours to allow the complete decay of the photodoping effect. Then, the procedure was repeated with the illumination carried out at a different  $T_{\text{dop}}$ . During the cool-down to  $T_{\text{dop}}$  we carefully checked that the  $\rho_{ab}$  vs.  $T$  curve was identical with the characteristics of the undoped sample to ensure that the sample was completely relaxed. Extreme care was taken to maintain the

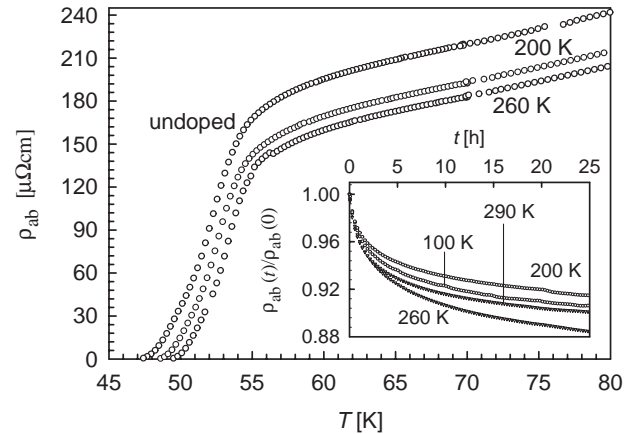


**Fig. 1.** The  $\rho_{ab}$  vs.  $T$  characteristics of  $\text{YBa}_2\text{Cu}_3\text{O}_x$  (sample R2) before and after photodoping for 25 hours at 200 K and at 260 K. The inset shows the time evolution of  $\rho_{ab}$  during the illumination at several temperatures.

experimental conditions unchanged throughout the entire sequence of measurements. Finally, the magnetoconductivity  $\Delta\sigma_B \equiv \rho_{ab}(B)^{-1} - \rho_{ab}(0)^{-1}$  was calculated and fitted to the theory of superconducting fluctuations (see Sect. 3).

## 3 Results

Figure 1 shows the  $\rho_{ab}$  vs.  $T$  characteristics of the sample R2 at  $B = 0$  in the non-illuminated (“undoped”) state and after photodoping at 200 K and 260 K. The photo-induced changes were smallest at 200 K (see the inset in Fig. 1, where the time evolutions of the normalized resistivity during the photo-excitation at various  $T_{\text{dop}}$  are shown), with the  $T_c$ -enhancement  $\Delta T_c = 1$  K, taken at the midpoint of the transitions. At  $T_{\text{dop}} = 260$  K, we observed the largest resistivity decrease and the largest  $\Delta T_c = 2$  K. These results agree well with our previous studies [5,12]. It should be noted that, despite the different  $\Delta T_c$ , the shapes of the characteristics in the photodoped states are very similar slightly above  $T_c$ . Larger differences were observed near room temperature [12].

In Figure 2, the temperature dependences of  $\Delta\sigma_B$  for the sample R2 in the undoped and photodoped states ( $T_{\text{dop}} = 260$  K) are compared. Inset in Figure 2 shows  $\Delta\sigma_B$  given as a function of the absolute temperature for a narrow interval above the superconducting transition. In the photodoped sample,  $\Delta\sigma_B$  is obviously larger than in the undoped sample. The main panel in Figure 2 displays the data as  $\Delta\sigma_B$  vs.  $\epsilon$  [ $\epsilon = \ln(T/T_c)$  is the reduced temperature], as convenient in studies of superconducting fluctuations. Due to the larger  $T_c$  of the photodoped sample, the both curves show different slopes for  $\epsilon \leq 0.1$ , but they are almost identical for  $\epsilon > 0.1$ . The plot in Figure 2 is sensitive to the choice of  $T_c$ . To estimate the influence of  $T_c$  on the results, we determined  $T_c$  in three different ways. The first method (A) was to fit the undoped sample data to the Aslamazov-Larkin theory of superconducting fluctuations, using  $\xi_c(0)$ ,  $\xi_{ab}(0)$  and  $T_c$

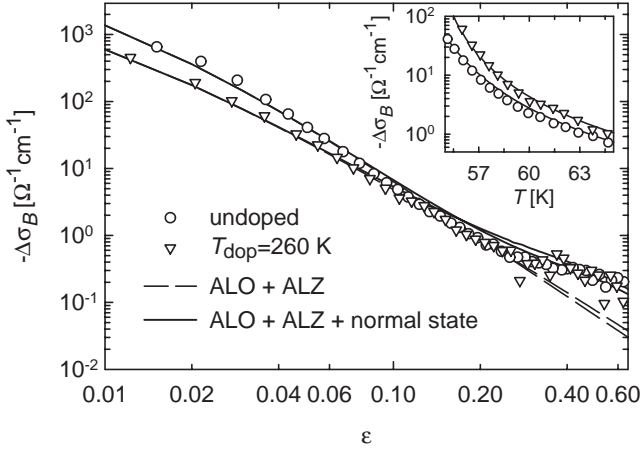


**Fig. 2.** Magnetoconductivity  $\Delta\sigma_B$  vs.  $\epsilon = \ln(T/T_c)$  of sample R2 in the non-illuminated and the photodoped states ( $T_{\text{dop}} = 260$  K). The broken lines are fits to the Aslamazov-Larkin theory of superconducting fluctuations, including orbital (ALO) and Zeeman (ALZ) contributions. The full lines additionally include the contribution of the normal-state carriers.

as adjustable parameters (the fitting procedure is described in detail in [13, 21, 22]). The  $T_c$  values of the photodoped samples were determined by adding the measured photoinduced shifts  $\Delta T_c$  to the undoped values. In the second method (B), all values of  $T_c$  (undoped and photodoped samples) were determined by applying the midpoint-of-transition criterion. Finally, in the third method (C),  $T_c$  was defined as that temperature within the transition region where  $\rho_{ab}$  changes its curvature. The fits according to the first method proved to be slightly better than the others and are therefore plotted in Figure 2. The agreement between theory (dashed line in Fig. 2) and experiment is very satisfying up to  $\epsilon \approx 0.2$  (corresponding to  $T \approx 65$  K). At higher temperatures, the discrepancies are, apparently, caused by the normal-state magnetoconductivity contribution, not included in the theory. To account for the latter, a correction using the measured transverse resistivity data was used (see [23]). Theoretical curves that include the normal-state contribution are plotted as full lines in Figure 2. It should be stressed, however, that the normal-state correction has a negligible influence on the values of fitted parameters. From the fits in Figure 2, we obtained  $\xi_c(0) = 0.07$  nm,  $\xi_{ab}(0) = 2.60$  nm, and  $T_c = 52.4$  K for the undoped sample R2, and  $\xi_c(0) = 0.19$  nm,  $\xi_{ab}(0) = 2.90$  nm, and  $T_c = 54.1$  K for R2 photodoped at 260 K. Table 1 lists superconducting properties,  $T_c$ ,  $\xi_{ab}(0)$ ,  $\xi_c(0)$ , and  $\xi_{ab}(0)/\xi_c(0)$  of the three studied samples in their non-illuminated (“undoped”) states.

In Figure 3,  $\xi_c(0)$  and  $\xi_{ab}(0)$ , normalized to their undoped values, and obtained by using method (A) to determine  $T_c$  are plotted as a function of  $T_{\text{dop}}$ . The uncertainty associated with the  $T_c$  determination method is indicated by the error bars in the figure. In all cases, the coherence lengths in the photodoped samples are larger than in the non-illuminated samples, but what is most interesting, in all studied samples, both  $\xi_c(0)$  and  $\xi_{ab}(0)$  increase monotonously with increasing  $T_{\text{dop}}$ , but the changes of

**Table 1.** Superconducting properties of the three studied samples before photodoping.  $\xi_{ab}(0)$  and  $\xi_c(0)$  are the in-plane and out-of-plane coherence lengths.  $T_c$  is the critical temperature determined by method (A), as described in the text.

sample	$T_c$ [K]	$\xi_{ab}(0)$ [nm]	$\xi_c(0)$ [nm]	$\xi_{ab}(0)/\xi_c(0)$
R1	50.6	2.5	0.07	35.7
R2	52.4	2.6	0.07	37.1
Y10	57.2	2.7	0.08	36.0

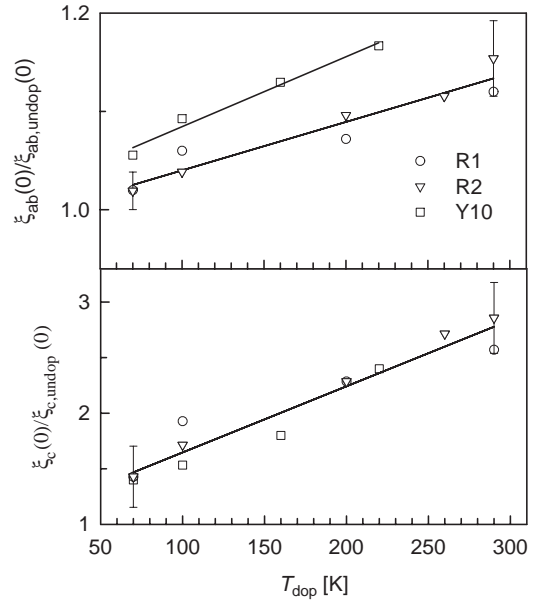


**Fig. 3.** Superconducting coherence lengths  $\xi_{ab}(0)$  (upper panel) and  $\xi_c(0)$  (lower panel) in three samples of  $\text{YBa}_2\text{Cu}_3\text{O}_x$  as a function of  $T_{\text{dop}}$ .  $\xi_{ab}(0)$  and  $\xi_c(0)$  were normalized to the values for the non-illuminated samples. The lines are guides to the eye. The error bars characterize the uncertainties of the plotted values due to alternatively determined  $T_c$ .

$\xi_c(0)$  are substantially larger than of  $\xi_{ab}(0)$ . As a consequence, the quantity  $\xi_{ab}(0)/\xi_c(0)$  that measures the electronic anisotropy of the superconducting carriers *decreases* with increasing  $T_{\text{dop}}$  (see Fig. 4). In the non-illuminated samples,  $\xi_{ab}(0)/\xi_c(0) = 36 \pm 2$ , which is reduced to about  $27 \pm 4$  by photodoping at 70 K, and to about  $16 \pm 2$  at 290 K. As in Figure 3, the error bars indicate the influence of the choice of  $T_c$  and suggest that the  $T_c$  determination method had only a minor significance on our results. It should be noted that the above results are qualitatively similar, but quantitatively significantly larger than that reported in our previous study [13]. In [13], photodoping was carried out at 150 K in a different experimental set-up (*e.g.*, a Xenon arc lamp was used).  $T_c$  enhancement in [13] was only about 0.5 K, demonstrating that the photodoping was less effective than in the present work.

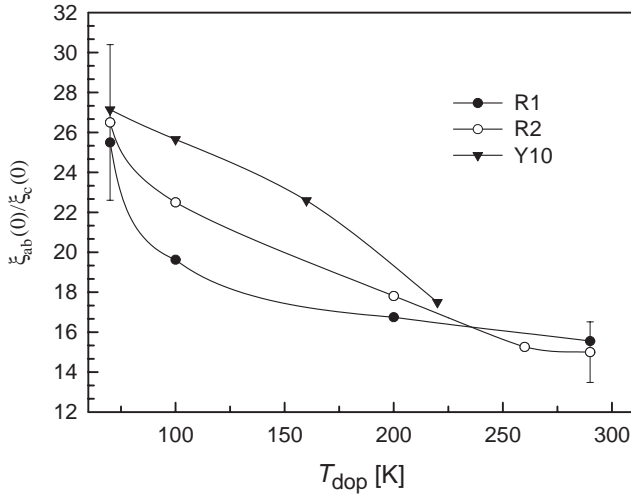


**Fig. 4.** Anisotropy of the coherence lengths,  $\xi_{ab}(0)/\xi_c(0)$  as a function of  $T_{dop}$ . The lines are guides to the eye.

## 4 Discussion

The results in Figures 3 and 4 demonstrate unambiguously that the superconducting properties of the photo-generated charge carriers in oxygen-deficient  $\text{YBa}_2\text{Cu}_3\text{O}_x$  depend on the temperature  $T_{dop}$  at which the photodoping is performed. The absolute values of  $\xi_{ab}(0)$  and  $\xi_c(0)$  increase during photo-excitation and this enhancement is increased as  $T_{dop}$  is increased, whereas the anisotropy  $\xi_{ab}(0)/\xi_c(0)$  decreases with the increase of  $T_{dop}$ . The reduction of anisotropy is expected from  $c$ -axis shrinking caused by photodoping [6,7], a phenomenon which is frequently used to support the so-called photo-assisted oxygen-ordering model [2,3,11]. Although this process is not unambiguously established yet, we also regard oxygen-ordering as the most plausible explanation, since a decrease of the lattice constants indicates a transformation of the system into a more ordered state. In contrast to the oxygen ordering, the other models proposed for photodoping assume randomly situated potential deformations in the CuO-chain layer of  $\text{YBa}_2\text{Cu}_3\text{O}_x$  arising from trapped electrons [1,24,25]. It seems hardly conceivable how such disordering processes could reduce the  $c$ -axis length. Assuming that the photo-induced contraction of the  $c$ -axis indicates oxygen-ordering, Figure 4 points that photodoping is connected with oxygen-ordering at *all* temperatures, and on top of it, this ordering process is more effective at large temperatures.

It is very instructive to compare the above results with the photo-induced changes of the normal-state transport properties. For this purpose, we have plotted in Figure 5 the normal-state anisotropy  $\rho_c/\rho_{ab}$  of  $\text{YBa}_2\text{Cu}_3\text{O}_x$  thin films grown on “tilted” substrates [15]. The figure shows  $\rho_c/\rho_{ab}(100\text{ K})$ ,  $\rho_c/\rho_{ab}(160\text{ K})$ , and at  $\rho_c/\rho_{ab}(290\text{ K})$ , normalized to the undoped values, as a function of  $T_{dop}$  and we note that  $\rho_c/\rho_{ab}$  also decreases with increasing  $T_{dop}$ . The essential difference between  $\xi_{ab}(0)/\xi_c(0)$  and  $\rho_c/\rho_{ab}$  is, however, that the former is *always* reduced by

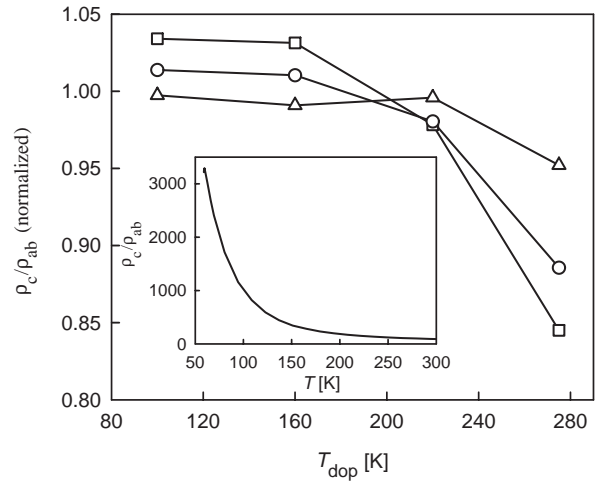


**Fig. 5.** Electrical normal-state anisotropy  $\rho_c/\rho_{ab}$ , taken at 100 K (squares), 160 K (circles), and 290 K (triangles), normalized to the undoped values, and plotted *vs.*  $T_{dop}$ . The lines are guides to the eye. The inset shows  $\rho_c/\rho_{ab}$  *vs.* temperature of the non-illuminated sample.

photodoping, whereas the behavior of the latter depends on  $T$  and on  $T_{dop}$ .  $\rho_c/\rho_{ab}(100\text{ K})$  and  $\rho_c/\rho_{ab}(160\text{ K})$  are both  $> 1$  at low  $T_{dop}$ , but  $< 1$  at high  $T_{dop}$ . At  $T = 290\text{ K}$ ,  $\rho_c/\rho_{ab}$  remains almost unchanged up to  $T_{dop} = 220\text{ K}$ , but falls also below 1 at higher  $T_{dop}$ . These observations strongly suggest that the photodoping, carried out at high  $T_{dop}$  tends to reduce the electronic anisotropy of  $\text{YBa}_2\text{Cu}_3\text{O}_x$  in the normal state as well as in the superconducting state. Both effects may be explained by the  $c$ -axis shrinking, which is expected to enhance the hopping rate for the normal-state carriers and to increase the overlap of the wavefunctions along the  $c$ -axis in the superconducting state. On the other hand, the normal-state anisotropy is obviously not only due to  $c$ -axis contraction, but is also affected by an additional process which enhances the anisotropy at low temperatures. The latter conclusion is not only drawn from Figure 5, but also from our recent studies [15] of the time evolution of  $\rho_c/\rho_{ab}$  during photodoping. In [15], we have observed that photodoping at low temperatures causes a persistent enhancement of  $\rho_c/\rho_{ab}$ , whereas at high temperatures there is a competition between a process that increases  $\rho_c/\rho_{ab}$  and another one that reduces  $\rho_c/\rho_{ab}$ . The second process seems to be attributed to oxygen-ordering, while the nature of the first process (increasing  $\rho_c/\rho_{ab}$  and dominating at low temperatures) remains questionable. From our present results (Figs. 4 and 5) as well as from the previous X-ray studies [6,7], carried out at low temperatures, it is inferred that the  $c$ -axis contraction occurs at *all* temperatures. The unknown process must, therefore, be able to increase the normal state anisotropy even though the  $c$ -axis shrinks. We can only speculate that a process similar to the so-called electron-capture mechanism [1,24,25], may introduce local lattice distortions in the CuO-chain layer in such way that the energy barrier for the incoherent  $c$ -axis transport is enhanced. Additionally, on a long-range scale, oxygen-ordering can occur, resulting

in an overall contraction of the  $c$ -axis. At high temperatures, the oxygen-ordering works more effectively (as shown in Fig. 5) and weakens the influence of the local distortions. On the other hand, the superconducting state is insensitive to local defects, so that  $\xi_{ab}(0)/\xi_c(0)$  is dominated by the  $c$ -axis contraction, in agreement with the results in Figure 4.

Another important aspect of the photodoping effect is very different behavior of  $\xi_{ab}(0)$  on photodoping as compared to chemical (oxygen) doping. In our 60-K samples,  $\xi_{ab}(0)$  is equal to 2.5 to 2.7 nm in the undoped states, and increases by about 10–15% through photodoping, in qualitative agreement with our previous results [13]. However, in 90-K  $\text{YBa}_2\text{Cu}_3\text{O}_x$  we have obtained  $\xi_{ab}(0) = 1.4$  nm [22]. Thus, oxygen doping reduces  $\xi_{ab}(0)$  substantially, whereas photodoping increases  $\xi_{ab}(0)$  (Fig. 3). Our previously raised argument (see [13]) that the photo-induced oxygen-ordering reduces the defect density in the material and thereby enhances  $\xi_{ab}(0)$  remains valid, but it requires an additional comment. If the oxygen order were to determine the values of the coherence lengths, then  $\xi_{ab}(0)$  in  $\text{YBa}_2\text{Cu}_3\text{O}_x$  should be larger for  $x = 7$  than for  $x = 6.5$ , because in the former a much higher degree of the oxygen order is achieved. However, this is not observed. Thus, not oxygen ordering, but the increase of the carrier concentration via the oxygen content must dominate and lead to the reducing effect on  $\xi_{ab}(0)$ . According to this concept, the larger value of  $\xi_{ab}(0)$  in 60-K  $\text{YBa}_2\text{Cu}_3\text{O}_x$ , as compared to 90-K  $\text{YBa}_2\text{Cu}_3\text{O}_x$ , is due to the reduced oxygen content, and is even further increased by the oxygen-ordering component of photo-excitation.

This work was supported by the Fonds zur Förderung der wissenschaftlichen Forschung, by the Jubiläumsfonds der Österreichischen Nationalbank, by the Bundesministerium für Unterricht und Verkehr, Austria, and by the US Office of Naval Research grant N00014-98-1-0080, Rochester. R.A. also acknowledges support from the Frank Horton Graduate Fellowship Program.

## References

- V.I. Kudinov, I.L. Chaplygin, A.I. Kirilyuk, N.M. Kreines, R. Laiho, E. Lähderanta, C. Ayache, *Phys. Rev. B* **47**, 9017 (1993).
- G. Nieva, E. Osquiguil, J. Guimpel, M. Maenhoudt, B. Wuyts, Y. Bruynseraede, M.B. Maple, I.K. Schuller, *Appl. Phys. Lett.* **60**, 2159 (1992).
- G. Nieva, E. Osquiguil, J. Guimpel, M. Maenhoudt, B. Wuyts, Y. Bruynseraede, M.B. Maple, I.K. Schuller, *Phys. Rev. B* **46**, 14249 (1992).
- K. Tanabe, S. Kubo, F. Hosseini Teherani, H. Asano, M. Suzuki, *Phys. Rev. Lett.* **72**, 1537 (1994).
- C. Stockinger, W. Markowitsch, W. Lang, W. Kula, R. Sobolewski, *Phys. Rev. B* **57**, 8702 (1998).
- K. Kawamoto, I. Hirabayashi, *Phys. Rev. B* **49**, 3655 (1994).
- D. Lederman, J. Hasen, I.K. Schuller, E. Osquiguil, Y. Bruynseraede, *Appl. Phys. Lett.* **64**, 652 (1994).
- K. Widder, J.Münzel, M. Göppert, D. Lierßen, R. Becker, A. Dinger, H.P. Geserich, C. Klingshirn, M. Kläser, G.Müller-Vogt, J. Geerk, V.M. Burlakov, *Physica C* **300**, 115 (1998).
- J. Watte, G. Els, C. Andrzejak, G. Güntherodt, V.Y. Moshchalkov, B. Wuyts, M. Maenhoudt, E. Osquiguil, R.E. Silverans, Y. Bruynseraede, *J. Supercond.* **7**, 131 (1994).
- V. I. Kudinov, *Physica B* **194**, 1963 (1994).
- E. Osquiguil, M. Maenhoudt, B. Wuyts, Y. Bruynseraede, D. Lederman, I.K. Schuller, *Phys. Rev. B* **49**, 3675 (1994).
- C. Stockinger, W. Markowitsch, W. Lang, W. Kula, R. Sobolewski, *Eur. Phys. J. B* **2**, 301 (1998).
- W. Göb, W. Lang, W. Markowitsch, V. Schlosser, W. Kula, R. Sobolewski, *Solid State Commun.* **96**, 431 (1995).
- W. Markowitsch, C. Stockinger, W. Lang, K. Bierleutgeb, J.D. Pedarnig, D. Bäuerle, *Appl. Phys. Lett.* **71**, 1246 (1997).
- C. Stockinger, W. Markowitsch, W. Lang, R. Rössler, J.D. Pedarnig, D. Bäuerle, *Physica C* **317-318**, 614 (1999) and C. Stockinger, W. Markowitsch, W. Lang, R. Rössler, J.D. Pedarnig, D. Bäuerle, *Phys. Rev. B* **60**, 7640 (1999).
- R. Sobolewski, L. Shi, T. Gong, W. Xiong, Y. Kostoulas, P.M. Fauchet, in *High-Temperature Superconducting Detectors: Bolometric and Nonbolometric*, edited by M. Nahum, J.-C. Villegier (SPIE, Bellingham, WA, 1994), Vol. 2159, pp. 110-120.
- W. Kula, W. Xiong, R. Sobolewski, J. Talvacchio, *IEEE Trans. Appl. Supercond.* **5**, 1177 (1995).
- H. Lengfellner, S. Zeuner, W. Prettel, K.F. Renk, *Europhys. Lett.* **25**, 375 (1994).
- S.T. Li, A. Ritzer, E. Arenholz, D. Bäuerle, W.M. Huber, H. Lengfellner, W. Prettl, *Appl. Phys. A* **63**, 427 (1996).
- D. Bäuerle, *Laser Processing and Chemistry* (Springer, Berlin 1996).
- W. Lang, W. Göb, W. Kula, R. Sobolewski, *Z. Phys. B* **98**, 453 (1995).
- C. Sekirnjak, W. Lang, S. Proyer, P. Schwab, *Physica C* **243**, 60 (1995).
- W. Lang, G. Heine, W. Liebich, X.L. Wang, X.Z. Wang, in *Fluctuation Phenomena in High Critical Temperature Superconducting Ceramics*, edited by M. Ausloos, A.A. Varlamov (NATO-ASI Series, Kluwer academic publishers, Dordrecht 1997), p. 81-90.
- N.M. Kreines, V.I. Kudinov, *Mod. Phys. Lett B* **6**, 289 (1992).
- J. Hasen, D. Lederman, I.K. Schuller, V.I. Kudinov, M. Maenhoudt, Y. Bruynseraede, *Phys. Rev. B* **51**, 1342 (1995).